Article:
Rayner, Peter J. and Duckett, Simon B. (2018) Signal Amplification by Reversible Exchange (SABRE):: From Discovery to Diagnosis. Angewandte Chemie International Edition. pp. 6742-6753. ISSN: 1433-7851

https://doi.org/10.1002/anie.201710406

Signal Amplification by Reversible Exchange (SABRE): From Discovery to Diagnosis

Peter J. Rayner[a] and Simon B. Duckett*[a]

Abstract: Signal Amplification by Reversible Exchange (SABRE) turns typically weak magnetic resonance responses into strong signals making previously impractical measurements possible. This technique has gained significant popularity due to its speed and simplicity. This minireview tracks the development of SABRE from the initial hyperpolarization of pyridine in 2009, to the point where 50% ^{1}H polarization levels have be achieved in a di-deuterio-nicotinate, a key step in the pathway to potential clinical use. Simple routes to highly efficient ^{15}N hyperpolarization and the creation of hyperpolarized long-lived magnetic states are illustrated. It finishes by describing how the recently reported SABRE-RELAY approach offers a route for *para*hydrogen to hyperpolarize a much wider array of molecular scaffolds, such as amides, alcohols, carboxylic acids and phosphates, than was previously thought possible. We predict that collectively these developments ensure that SABRE will significantly impact on both chemical analysis and the diagnosis of disease in the future.

1. Introduction

Nuclear Magnetic Resonance (NMR) and Magnetic Resonance Imaging (MRI) are now ubiquitous techniques that are used in the study of molecules and materials despite an inherent insensitivity. Classically, the small Boltzmann derived spin energy level population difference is overcome through the use of large magnetic fields, increased sample concentrations and extended signal averaging. However, these approaches have both time and cost implications, and for this reason, essentially all current clinical MRI applications make use of a water signal due to its high *in vivo* concentration. Thus, hyperpolarization methods that create a non-Boltzmann population distribution of magnetic spins are highly desirable and have now begun to influence biomedical imaging and disease diagnosis.[1] Spin Exchange Optical Pumping (SEOP) and Dynamic Nuclear Hyperpolarization (DNP) are two of the most clinically developed approaches, having been successfully used for the study of lung physiology and prostate cancer metabolomics respectively.[1c, 1d, 2] Hence, hyperpolarized MRI is predicted to play a growing role in human health.[1a, 3]

In addition, given the widespread use of NMR for the characterization of materials in solution, hyperpolarization also opens up potential routes for analysis where only small amounts of analyte are available.[4] Such methods are likely to be of great importance for the detection and identification of trace impurities in the pharmaceutical pipeline. Furthermore, the identification of transient reaction intermediates involved in catalytic processes reflect a further area where hyperpolarization studies might be expected to aid the improvement of reaction outcomes and thus, reduce the environmental impact of industrial processes.[5]

An alternative and simple route to nuclear spin polarization involves the addition of singlet state based *para*-hydrogen (p-H_2) to an unsaturated center, collectively termed *Para*Hydrogen Induced Polarization (PHIP).[6] The potential clinical uptake of PHIP techniques have been hindered by the need for chemical change - commonly hydrogenation of organic molecules such as alkynes and alkenes – which limits the range of suitable substrates.[7] Recently, the use of cleavable, unsaturated molecular tags, including propargyl esters, has broadened the scope of the PHIP method to include access to pyruvate, acetate and even lactate for the monitoring of metabolism *in vitro*.[8]

In 2009, the PHIP technique termed Signal Amplification by Reversible Exchange (SABRE) allowed access to hyperpolarized substrates without changing their chemical identity.[9] While SABRE releases the latent polarization in p-H_2 by binding it to a metal catalyst, the concurrent binding of a substrate molecule allows it to become hyperpolarized by transfer through the scalar coupling network[7, 10] and dissociation allows the build-up of polarized substrate in solution by the cycling of the steps as depicted in Scheme 1. We set out here to show how SABRE reflects a rapid and efficient route to hyperpolarization that we predict will impact favorably on many areas of science in the future.

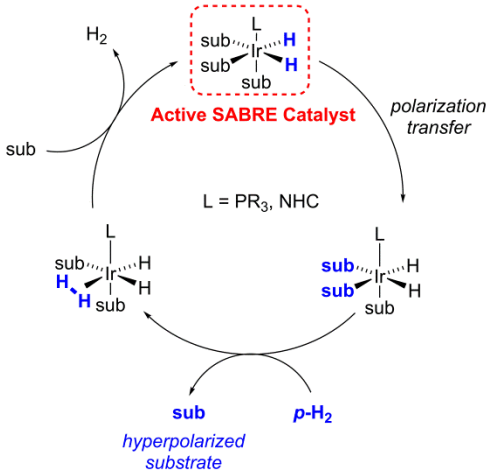

Scheme 1. Schematic representation for the SABRE catalytic cycle in which p-H_2 hyperpolarizes a target substrate (sub).

2. Development of SABRE Catalysis

SABRE is a catalytic process where in the transfer of latent magnetization from p-H_2 proceeds to a target substrate. To achieve this effect, a metal center acts as a scaffold to temporarily bring together the substrate and p-H_2 in the form of hydride ligands. At low magnetic field, polarization is

[a] Dr. P J, Rayner, Prof. Dr. S B Duckett
Centre of Hyperpolarisation in Magnetic Resonance
Department of Chemistry, University of York
Heslington, YO10 5DD, U.K.
E-mail: simon.duckett@york.ac.uk

spontaneously transferred through the scalar coupling network,[10-11] though in-high-field transfer using radio frequency (*r.f.*) methods have also been applied.[12] A number of theoretical descriptions[7, 9-11, 13] for the SABRE technique have been reported.

2.1. Theoretical Descriptions of SABRE

The SABRE phenomenon was originally described using a density matrix theory approach based on a model four-spin system derived from two spins which originate in *p*-H_2 and two that originate in the bound substrate.[10] The low field evolution of the polarization as a function of magnetic field was modelled and the effect of transport into the magnet considered. The analytical solution predicts that scalar coupling in the SABRE catalyst results in the transfer of spin order between the *p*-H_2 derived hydride ligands and the two additional bound nuclei. These nuclei were found to retain enhanced populations of visible longitudinal single spin (the normal Zeeman polarization) and two-spin order terms after substrate dissociation. However, the associated zero quantum terms were stated to reflect the creation of singlet states that would be preserved in ultra-low field. Unfortunately, while being accurate, this model's reliability depends critically on several very small *J*-couplings that are hard to measure.

A complementary method based on level anti-crossings (LACs) yields analogous but more qualitative results, whilst providing a much clearer and intuitive picture of the origin of SABRE polarization.[11, 13a] A LAC arises at a magnetic field where two energy levels would cross in the absence of spin-spin coupling. For SABRE, efficient mixing of the corresponding substrate and *p*-H_2 derived spin-states therefore occurs when substrate and hydride resonance frequency differences match the difference between the mutual hydride spin couplings and the sum of one quarter of their mutual couplings to substrate.[13c] Hence spin order transfer efficiency depends explicitly on the scalar coupling network within the catalyst and the magnetic field experienced at the point of polarization transfer. Thus, this method has the benefit of enabling the rapid prediction of the optimum magnetization transfer field for a particular substrate.

However, as SABRE is a dynamic process, the effect of chemical exchange of *p*-H_2 and the substrate at the catalyst need to be considered. Furthermore, spin state relaxation during this process tempers the build-up of SABRE derived polarization in solution. An analytical model that combines kinetics and nuclear spin evolution has been presented which addresses these concerns.[13b] This model predicted that optimal SABRE transfer, in the low field regime, occurs when the rate constant for substrate dissociation is on the order of the spin mixing frequency at a LAC. Conversely, the substrate dissociation rates should be as fast as possible for high field SABRE. Additionally, the relative concentrations of *p*-H_2, substrate and catalyst are important, with large signal enhancements resulting for low substrate-to-catalyst ratios and high *p*-H_2-to-catalyst ratios. The authors conclude that relaxation within the active catalyst can inhibit efficient polarization build up.

Peter Rayner received his MChem degree from the University of York in 2009. He then joined the group of Prof. P. O'Brien where he studied asymmetric synthesis using α-functionalized organometallic reagents. After obtaining his Ph.D. in 2013, he moved to the group of Prof. S. Duckett where he is currently developing the SABRE hyperpolarization method towards clinical applications.

Simon Duckett is the Director of the Centre for Hyperpolarization in Magnetic Resonance. His group studies and develops hyperpolarization techniques with a view to translation into the clinic. In 1990, he was awarded a D.Phil. from the University of York and afterwards undertook postdoctoral work with Prof. W. D. Jones and Prof. R. Eisenberg at the University of Rochester. He has authored over 90 publications on the *para*hydrogen effect.

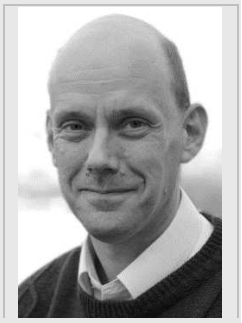

Both the steady-state and dynamic behavior of the SABRE process have been considered using a strategy that takes into account spin-evolution in the catalyst and substrate exchange.[13c] This method allows for multi-spin systems, time dependent SABRE polarization and polarization formed through *r.f* irradiation. This report also includes a comparison of the theoretical descriptions of the SABRE effect.

Overall, the reported theoretical descriptions allow us to define the key components needed for optimal SABRE catalysis; the lifetime of the active SABRE catalyst must be on the appropriate timescale for efficient polarization transfer; the size of the spin-spin coupling between the *p*-H_2 derived hydride ligands themselves and the NMR active nuclei in the substrate must be large relative to the timescale of relaxation; the polarization transfer field (PTF) at which the catalysis is undertaken must reflect the matching condition associated with optimal transfer. These factors have been explored and harnessed through an array of experimental studies whose chronology can predate these theoretical predications.

2.2. Ancillary ligand effects on SABRE complex lifetime

In fact the reversible binding of the substrate and *p*-H_2 to the metal complex were found experimentally to be crucial to efficacious SABRE. If these binding interactions are too strong, and become irreversible, then efficient polarization is suppressed as the necessary *p*-H_2 addition is stopped. Likewise, if these interactions are too weak, then the active SABRE catalyst can become unstable leading to rapid depletion of *p*-H_2,[14] inefficient polarization transfer[13c] or, at worst, the catalysts decomposition. As such the development of metal complexes that mediate reversible exchange on an appropriate timescale has received much attention.

The initial SABRE observations utilized the pre-catalyst $[Ir(COD)(PCy_3)(py)]BF_4$ (where COD = *cis*,*cis*-1,5-cyclooctadiene, Cy = cyclohexane and py = pyridine) to mediate polarization

transfer.[9] The active complex in this case is formed by the oxidative addition of H_2 in the presence of excess pyridine to give $[Ir(H)_2(PCy_3)(py)_3]BF_4$. The small scalar couplings between the hydride ligand and *ortho*-pyridine protons[15] were sufficient to allow spontaneous magnetization transfer to take place at low magnetic field.[16] It was rapidly realized that the identity of the phosphine ligand played an important role, with the corresponding PCy_2Ph derived catalyst proving to be far superior.[16] This improvement was due to the fact that the steric bulk of the phosphine promoted substrate loss whilst its strong electron donating properties promoted H_2 exchange.

It was the discovery that by replacing the phosphine ligand with an *N*-Heterocyclic Carbene (NHC) which unlocked the large polarization levels that are now associated with SABRE.[17] In fact, the air stable pre-catalyst [IrCl(COD)(IMes)] (where IMes = 1,3-bis(2,4,6-trimethylphenyl)imidazol-2-ylidine) resulted in ~8.1% polarization for pyridine compared with 2.5% for the phosphine catalyst. This improvement was found to be associated with the increased rate of pyridine dissociation from the active catalyst $[Ir(H)_2(IMes)(py)_3]Cl$ and the promotion of H_2 exchange. Exchange Spectroscopy (EXSY) was used to quantify the rate constant for pyridine dissociation in $[Ir(H)_2(IMes)(py)_3]Cl$ as 23 s^{-1},[18] which is significantly faster than that of the phosphine derived catalyst $[Ir(H)_2(PCy_3)(py)_3]Cl$ which had a pyridine dissociation rate constant of just 0.45 s^{-1}.[16]

Substrate dissociation is vital to the 'refreshing' of *p*-H_2 within SABRE catalysis as shown in Scheme 1. In the case of IMes derived catalysts, this leads to the transient formation of $[Ir(H)_2(\eta^2\text{-}H_2)(IMes)(py)_2]Cl$ which can rearrange to expel H_2 and bind the substrate in either an associative or dissociative manor to complete the catalytic cycle. Density Functional Theory (DFT) has been used to confirm these proposed intermediates.[17]

The identity of the NHC ligand can also be modified to vary the lifetime of the active complex. For example, the sterically bulky SIMes or IPr ligands of Figure 1 yield increased rates of pyridine dissociation as a consequence of the change in $\%V_{bur}$.[18] Despite over 10 commercially available NHC ligands used for the SABRE polarization of pyridine,[18-19] to date [IrCl(COD)(IMes)] remains the most impressive mediator of polarization transfer. This optimum activity is common across a range of heterocyclic motifs although rare examples exist where this is not the case.[20]

Thus far, no quantifiable correlation between the steric and electronic properties of the NHC ligands and polarization levels has been established; however aromatic NHC ligands typically show improved performance.[19] This reflects the complexity of the SABRE transfer step, although recently the π-accepting ability parameter[21] has been shown to offer better insight into how the NHC ligand influences the rate of pyridine exchange.[22]

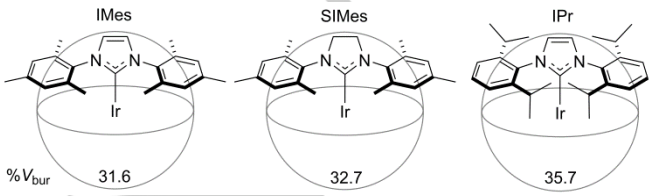

Figure 1. Structures of NHC ligands used for SABRE catalysis.

Other SABRE catalysts have been shown to undergo such non-hydrogenative transfer of polarization including the bidentate NHC-phenolate (**1**),[23] an iridium PNP-pincer (**2**)[14] and an iridium cyclooctene complex (**3**)[24] shown in Figure 2, however signal gains were reduced when compared to [IrCl(COD)(IMes)].

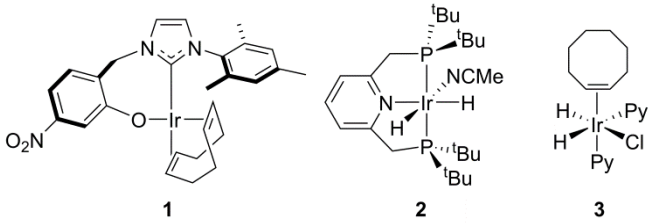

Figure 2. Structures of alternative ligands used for SABRE catalysts

In summary, catalyst identity is critical for efficient SABRE and can be used to control the polarization outcome. Looking forward, it may be possible to further modulate the complex lifetimes through ligand development which could be the key to expanding the substrate range amenable to the SABRE method.

2.3. Effect of polarization transfer field on SABRE catalysis

The magnetic field at which SABRE catalysis is conducted has been shown to determine the magnitude of substrate polarization. For SABRE transfer to ^1H nuclei, the magnetic field at which maximum polarization transfer is observed is caused by the LAC point as determined by the hydride-hydride scalar coupling in the active SABRE catalyst[11] or by optimal spin evolution within the density matrix model.[10] Both theoretical approaches provided comparable conclusions. The hydride-substrate coupling then allows polarization to transfer and Tessari *et al.* have shown experimentally that a typical $^4J_{HH}$ coupling is ~1.2 Hz (Figure 3.).[15] As such, for transfer to ^1H-nuclei, optimal polarization transfer is usually observed in the ~5-8 mT range[17, 25] and the PTF can be accurately controlled using an automated flow system.[26]

Polarization can also be transferred to heteronuclei bound directly to the catalyst via a $^2J_{HX}$ scalar coupling. This refinement has been exemplified for both ^{15}N[27] and ^{31}P[28] hyperpolarization. When a $^2J_{HX}$ scalar coupling is used, the optimum transfer field can now be in the region of ~0.2-0.4 μT which is achieved by conducting the SABRE catalysis inside a μ-magnetic shield.[27a] This protocol has been termed "SABRE-SHEATH" (Signal Amplification by Reversible Exchange-in SHield Enables Alignment Transfer to Heteronuclei) and its scope is discussed in detail later.

A drawback of conducting the SABRE polarization transfer in low magnetic fields is the requirement for fast transfer into high field where detection takes place. Alternate approaches use radio frequency (*r.f.*) methods to drive polarization transfer at high field. Thus, immediate detection and recycling is possible which provides a simple route to rapid repetitive measurements.

High-field SABRE was used in 2009 when *p*-H_2 derived magnetization was transferred to pyridine-^{15}N using an INEPT

based procedure.[12a] Methods to transfer polarization have since been developed that fulfil the LAC demands of SABRE through *r.f.* excitation.[12b, 29] This route has been applied to a range of substrates and ^{1}H signal enhancements of *ca*. 360-fold at 9.4 T have been achieved. Recently, the Alternating Delays Achieve Polarization Transfer (ADAPT)[30] sequence has been applied to to SABRE to give a ^{15}N signal gain of nearly 1000-fold at 11.7 T in just 1.6s.[31]

Alternatively, high-field transfer can be achieved using low-power continuous-wave pulses, in the LIGHT-SABRE (Low Irradiation Generation of High Tesla-SABRE) method.[12c] This approach has been used with ^{15}N-labelled pyridine and yielded ^{15}N signal enhancements of *ca*. 480-fold at 9.4 T. interestingly, as large resonance frequency differences can be overcome LIGHT-SABRE is applicable to any coupled pair of nuclei.

2.4. Use of a co-ligand in SABRE catalysis

As discussed, in order for *p*-H_2 to be harnessed its symmetry must be broken. High symmetry SABRE catalysts of the type $[Ir(H)_2(IMes)(substrate)_3]^+$ actually rely upon magnetic inequivalence for polarization transfer. However, by adding a co-ligand it is possible to form complexes of type $[Ir(H)_2(IMes)(substrate)_2(co\text{-}ligand)]^+$. In this scenario, polarization transfer results from both coupling and chemical asymmetry.. As the strength of the hydride-hydride and hydride-substrate couplings and catalyst lifetimes can be changed by varying the complex, tunable hyperpolarization efficiency results from both situations, although, in the latter case, transfer into the axial ligands is therefore possible. A number of examples have utilized an equatorially bound co-ligand, such as acetonitrile, to break the chemical symmetry of the SABRE active catalysis.[20, 23b, 32] In this case both acetonitrile and the target substrate are hyperpolarized. An alternative approach utilized a fully deuterated isotopologue of the targeted SABRE substrate as a co-ligand.[25, 32-33] Here, the co-ligand does not receive visible polarization itself and has the effect of focusing the polarization into the ^{1}H-sites on the target substrate. This method has yielded almost double the polarization level that could be achieved in the absence of the co-ligand.

A co-ligand is also required for substrates whose binding is too weak to stabilize the active catalyst or when a substoichiometic amount of substrate is present.[4e, 34] A common co-ligand in these situations is 1-methyl-1,2,3-triazole, as it has a higher affinity for binding to the complex than the solvent, has favorable lifetimes for SABRE and it's ^{1}H NMR signals do not overlap with those of the substrates that were studied.

2.5. Effect of the catalyst on relaxation rates

The rate of relaxation of the SABRE induced magnetization is also important if it is to survive to the site of a delayed measurement. It has been consistently shown across a range of substrates that, in the presence of the SABRE catalyst and H_2, the effective T_1 value of free substrate decreases.[18, 33] The measured T_1 values of the free substrate is therefore a weighted average of the material in bulk solution and that bound to the catalyst due to the reversible exchange process.[13b] By cooling the SABRE reaction to 263 K, ligand dissociation can be quenched, allowing relaxation rates for the substrate whilst bound to the catalyst to be measured. T_1 relaxation times of 0.5-2 s were observed for methyl 4,6-d_2-nicotinate which is a dramatic reduction of the T_1 value of the free material which is over 1 minute.[33]

In order to reduce this effect a number of approaches have been taken. First, by increasing the substrate concentration relative to the catalyst the equilibrium contributions of the free and bound substrate change and thus, the effective T_1 values increase.[18] However, this typically also leads to reduced enhancement values being observed. Alternatively, deuterium labelling of the NHC ligand has been shown to increase the lifetime of substrate polarization whilst bound to the metal center[20, 23b, 33, 35] and has led to the observed ^{1}H-polarization levels increasing by ~150% in methyl 4,6-d_2-nicotinate. This isotopomeric NHC ligand may also have the dual effect of not being able to receive polarization itself, and thus removes a further possibility for spin-dilution. A final option to extend the substrate relaxation time is through the addition of a chelating ligand, such as phenanothroline, after the SABRE polarization is complete. This process quenches the active SABRE catalyst thereby preventing the reversible exchange of the substrate and returns its T_1 values to normal which allows detectable polarization to remain visible for a longer time period.[36] However, this approach does not allow for re-hyperpolarization.

3. ^{1}H-SABRE Polarization

SABRE induced polarization of ^{1}H-nuclei is by far the most extensively studied to date due to the very high natural abundance, high gyromagnetic ratio and ubiquity in a range of naturally occurring and drug molecules. It also has the benefit of being directly observable on any existing hospital scanner which may lead to facile clinical translation.

3.1. Scope of ^{1}H SABRE Polarization

Typically Lewis basic nitrogen containing molecules such as *N*-heterocycles and nitriles[32] are most effective for ^{1}H-SABRE polarization although there are also a few successful examples of polarization transfer to sulfur heterocycles.[37] Substituted pyridyl substrates have proved to be particularly efficacious to SABRE and ^{1}H polarization levels of up to 50% have been reported.[33] More complex substrates have also been shown to be amenable to SABRE with molecules with multiple ligation modes[20, 38] and a number of biologically significant molecules such as nicotinamide,[33] vitamin B_3,[39] adenosine[40] and the tuberculosis drug, isoniazid showing good signal gains.[35, 41] It has also been shown that polarization efficiency is decreased if no $^4J_{HH}$ coupling is present in the active catalyst and a smaller $^{5/6}J_{HH}$ coupling has to be utilized instead.[33] These couplings are depicted in Figure 3 for the model catalyst $[Ir(H)_2(IMes)(py)_3]^+$.

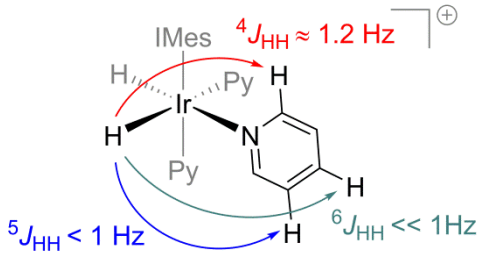

Figure 3. Representation of the scalar couplings between the hydride ligand and protons in the substrate molecule for $[Ir(H)_2(IMes)(py)_3]Cl$.

3.2. Effect of selective deuteration on substrate polarization and relaxation rate

A well-established route to improve the efficacy of hyperpolarization techniques is the use of selective deuteration of the substrate.[42] When applied to the SABRE technique, 3,4,5-d_3-pyridine showed improved performance over its *protio* analogue.[17, 43] A detailed study that probed the optimal deuteration pattern has been reported for nicotinamide and methyl nicotinate.[33] Placement a proton *ortho* to the nitrogen binding site was shown to be optimal for efficient polarization transfer but coupling to a remote proton was optimal for a long magnetic state lifetime. These structures are shown in Figure 4 and have up to 5 times greater T_1 values and delivers 4-fold improvement in polarization level. Similar improvements have now also been reported for the Tuberculosis drug isoniazid and its derivatives.[35]

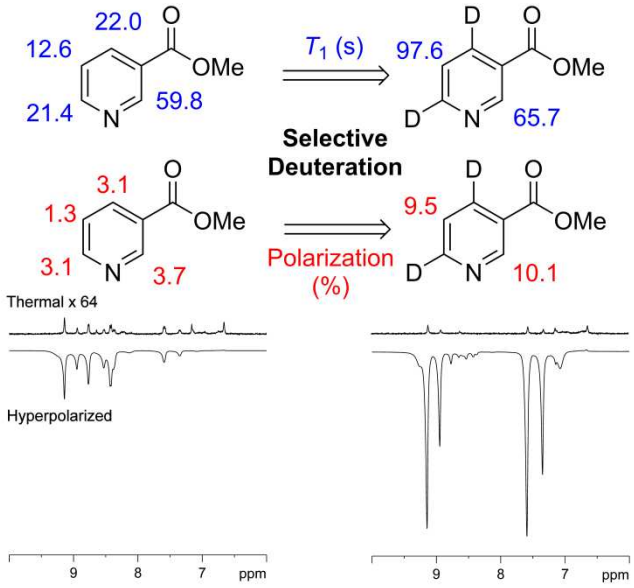

Figure 4. Comparison T_1 and polarization values for methyl nicotinate and its optimally deuterated isotopologue with their ^{1}H NMR thermal (top, x64 expansion) and hyperpolarized (bottom) spectra.

3.2. SABRE derived ^{1}H-singlet states

SABRE harnesses the long lived single state of *p*-H_2 as its source of polarization. In this context, singlet states are non-magnetic spin isomers of a coupled spin-1/2 pair which are immune to external dipolar coupling. It is therefore possible to identify other molecules where two almost identical protons exist in a single state as detailed by Levitt.[44] The SABRE technique can hyperpolarize such states, as was exemplified for the strongly coupled ^{1}H-pair in 2-aminothiazole[45] where the singlet state was accessed in 90% efficiency by rf-methods and using a spin-lock as pioneered by Levitt.[44] This approach has also been applied to derivatives of nicotinamide and pyrazinamide that have isolated spin-pairs through selective deuteration.[46]

The current state of the art utilizes a pyridazine based ^{1}H-spin pair that exhibit a $\Delta\delta$ of only 1 Hz despite having a strong $^3J_{HH}$ coupling.[47] As a consequence the state lifetime was observed to be over 4 minutes at low field and a SABRE hyperpolarized signal could still be observed 15 minutes after polarization transfer. This method shows great potential for progression towards clinical applications as the polarization can be stored in long live singlet state prior to injection and then subsequently observed *in vivo*.

4. ^{15}N-SABRE Polarization

Hyperpolarization of ^{15}N-nuclei offers an interesting alternative to ^{1}H-nuclei due to their relaxation times being typically longer. An area of rapid development over the past five years has been the direct polarization transfer to ^{15}N at low μT magnetic fields.[48] This SABRE-SHEATH method exploits the strong ^2J-coupling between the hydride ligands and a ^{15}N donor atom in the active catalyst.[27a]

4.1. Scope of ^{15}N-SABRE Polarization

The SABRE-SHEATH method has polarized a broad range of substrates that include *N*-heterocycles,[27b, 49] nitriles,[49a] Schiff bases,[50] diazene[49a] and diazirines.[34, 51] The antibiotic metronidazole has also been polarized with levels of over 20% and may lead to assessment of its *in vivo* fate.[52] ^{15}N-SABRE induced polarization has also been observed using permanent 1 T magnets[49a] and makes possible the polarization of neat liquids.[53]

5.2. $^{15}N_2$ Diazirines as Molecular Imagining Tags

More recently, SABRE has been applied to the hyperpolarization of $^{15}N_2$ diazirines, shown in Figure 5, which can be used as biocompatible molecular tags without significantly modulating biological function.[51] Interestingly, the type of polarization that was created can be selected simply by changing the magnetic field at which the SABRE process occurs. As such, polarization transfer at ca. 6 mG gave Z-magnetization (triplet state) with up to 5% polarization and a decay constant of ca. 6 min. Alternatively, the singlet state can be populated at almost any magnetic field because the coupling between the hydrides of the active catalyst, and the coupling between the $^{15}N_2$-diazirine are almost equal (J_{HH} = 10 Hz, J_{NN} = 17.3 Hz).

SABRE induced singlet polarization of ≈ 3% with a decay constant of 23 min was observed at 120 G.

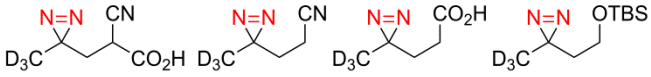

Figure 5. Structure of diazirines polarized using SABRE

The original reported diazirine contained two sites for potential ligation; the diazirine and nitrile functionalities. However, this has been shown to be unnecessary for efficacious $^{15}N_2$ polarization transfer.[34] Instead, addition of a Lewis basic additive (e.g. pyridine, MeCN, D_2O) sufficiently stabilizes the SABRE catalyst to give monodentate diazirine species. This important breakthrough may open the door to the use of diazirine tags for bimolecular imaging or a wide range of biological relevant targets in the future.

5. Polarization of Other Heteronuclei

5.1. ^{13}C-SABRE hyperpolarization

The hyperpolarization of ^{13}C nuclei has been the predominant choice for *in vivo* DNP studies due to its greater natural abundance than ^{15}N and typically long relaxation times.[1c, 1d, 54] However, the development of ^{13}C-SABRE has been hindered in part due to low polarization levels. When SABRE was employed for the polarization of nicotinamide at natural abundance, all six ^{13}C resonances were visible[26] whilst when the nicotinamide carbonyl was isotopically enriched a 65-fold enhancement at 9.4 T has been reported.[43] In 2015 Truong *et al*. probed the feasibility of transfer of SABRE-SHEATH induced polarization of ^{13}C in pyridine-^{15}N however enhancements were less than 10-fold at 9.4 T.[27b] More recently the hyperpolarization of pyridine-^{15}N was revisited and ^{13}C-polarization levels of ca. 4.4% were reported.[55] These improvements in SABRE efficiency are due to the utilization a μT polarization transfer field and optimization of temperature and concentration. Interestingly the ^{13}C-polarization observed in pyridine-^{14}N was significantly lower than its ^{15}N isotopologue. The authors concluded that this was due to significant quadrupolar ^{14}N-relaxation in the μT fields used during the study, which may inform the design of SABRE contrast agents in the future.

SABRE induced polarization of ^{13}C nuclei has also been stored in long lived states which have been accessed in a series of substituted pyridazines *via* either the breaking of their magnetic or chemical symmetry by synthetic design.[56] When magnetic inequivalence, due to the distinct scalar couplings between the carbon and proton nuclei, was utilized a ≈2.0% polarization level was observed in conjunction with a singlet lifetime of nearly 2 minutes at low field. It is likely that the polarization is transferred both directly and *via* the vicinal ^{1}H-nuclei as when they are replaced with deuterium the polarization dropped to ≈1.3%. When chemical inequivalence is used to access the singlet state by introduction of a CD_3 group to the phenyl ring, the singlet state lifetime was extended to over 3 minutes, though the polarization was reduced to ≈0.5%. This allowed a signal to be observed over 10 minutes after the SABRE catalysis was conducted. Functionalized acetylenes have been polarized under SABRE-SHEATH conditions to give up to 0.12% polarization at 8.5 T in conjunction with signal lifetimes of up to ~1.95 minutes at 0.3 mT. [57] This report utilizes the direct hydride-^{13}C couplings found in the active catalyst and multiple binding modes were found to be possible.

5.2 ^{31}P-SABRE Hyperpolarization

Polarization transfer to ^{31}P nuclei was initially seen when they feature as ligands on the SABRE catalyst and hence exhibit a direct coupling to *p*-H_2 derived hydride ligands.[23b] However, due to the strength of Ir-P bonds, reversible exchange did not occur at room temperature. In order to induce SABRE polarization into the phosphine ligands, Zhivonitko *et al*. heated a solution of $(PPh_3)_3Ir(H)_2Cl$ in toluene to 60 °C. Bubbling *p*-H_2 through the solution in a 1 μT magnetic field gave a 120-fold enhancement at 7 T.[28] This could be further improved by heating the solution to 80 °C where a 260-fold enhancement was now observed due to improved kinetic parameters. Hyperpolarized ^{31}P images of a phantom were also recorded under these conditions.

SABRE induced hyperpolarization of ^{31}P nuclei was also shown for a range of phosphorus substituted *N*-heterocycles where up to a 3588-fold enhancement at 9.4 T resulted.[58] This example involved indirect transfer to ^{31}P *via* ^{1}H nuclei on the pyridyl ring with the optimum PTF being 45 G and could be conducted at room temperature. This technique allowed for the polarization of a phosphine, a phosphine oxide, a phosphine sulfide and a phosphonate ester.

As a multitude of transition metal catalysts contain phosphine derived ligands, these techniques may open to door to NMR monitoring of low concentration reactive intermediates that may not be visible under standard NMR conditions.

5.3 ^{19}F-SABRE Hyperpolarization

The SABRE induced hyperpolarization of ^{19}F nuclei was initially reported for 3-fluoropyridine in 2009 though enhancement factors were not quoted.[9] More recently the polarization of 3-fluoropyridine was revisited with a view to developing ^{19}F molecular imaging probes.[59] Here, polarization levels of up to ≈ 0.28% (93-fold enhancement at 9.4 T) were observed. On addition of concentrated $HCl_{(aq)}$ to the solution, a 10 ppm ^{19}F chemical shift difference was reported, however, the enhancement was reduced to 13-fold due to extended sample handling times. Despite potential benefits for biomedical translation of ^{19}F molecular imaging, such as using the ^{1}H-channel on existing hospital MRI scanners and no biological background signal, the ^{19}F nucleus in 3-fluoropyridine has a T_1 value of just 10.3 s at 9.4 T and therefore perhaps precludes its use for *in vivo* imaging techniques. This highlights the need for the development of novel ^{19}F contrast agents with extended lifetimes.

5.4 ^{29}Si and ^{119}Sn-SABRE Hyperpolarization

^{29}Si and ^{119}Sn have also been shown to polarize by reversible exchange with *p*-H_2.[60] This approach again used relayed polarization from adjacent ^{1}H nuclei with optimal transfer occurring at 20 G to give over 200- and 700-fold signal gains at 11.7 T for ^{29}Si and ^{119}Sn respectively. As silyl and stannyl reagents play a prominent role in synthetic chemistry, typically as protecting groups or coupling partners, this opens the door to monitoring and identifying transient intermediates by NMR spectroscopy during chemical transformations.

6 Analytical Applications of SABRE

SABRE has found a wealth of applications in analytic sciences, whereby the improved signal strength allows for previously impractical measurements to be made in seconds. It is particularly advantageous for investigating analytes that are in low concentrations in solution.[4e, 61] For example, a solution containing just 2 µmol of quinoline was hyperpolarized using SABRE in an automated flow system which allowed for the collection of ^{13}C, ^{1}H and NOE data in addition to the 2D techniques, COSY AND HMBC.[61] SABRE can also be used to acquire 2D spectra utilizing FAST-NMR methods.[62] This has led to ultrafast COSY being recorded in under 1 s.[4a]

A limitation of low concentration measurements is that the active SABRE catalyst typically requires three substrate molecules to bind to the iridium center. Therefore, at substoichiometric amounts of substrate, the SABRE effect is prohibited. To overcome this, it is possible to use 1-methyl-1,2,3-triazole as a co-ligand to stabilize the catalyst.[4e] Importantly, it was noted that at substoichiometric substrate levels there was a linear relationship between substrate concentration and signal enhancement. This phenomenon has been exploited for the quantitative analysis of complex mixtures in single scan SABRE polarized ^{1}H NMR spectra.[63] These techniques have been applied to the study of analytes within biofluids[4d] and could allow for wider detection of drug metabolites in urine samples in the future. Low concentration analytes have also been detected by utilizing continuous SABRE hyperpolarization at high magnetic fields.[4f] More recently, Reile *et al*. have described the resolution of 6 dilute analytes by SABRE hyperpolarization coupled with Diffusion Ordered Spectroscopy (DOSY).[64]

7. Development of SABRE catalysis towards *in vivo* applications

7.1. SABRE catalysis in aqueous solutions

The majority of SABRE polarization studies have been conducted in methanol-d_4 or ethanol-d_6 solution however some examples using other organic solvents are reported.[23a, 41] Whilst, the biocompatible ethanol-d_6:D_2O is suitable for SABRE polarization,[43] T_1 relaxation values decrease in solvent mixtures when compared to the neat solutions.[33] Direct SABRE polarization in pure water is therefore desired, however the poor solubility of [IrCl(COD)(IMes)] in aqueous media needs to be overcome in order to achieve this goal.

One such method is to form the active SABRE catalyst by reaction with *p*-H_2 and a substrate in an organic solvent as this chemical change leads to improved aqueous solubility. Zeng and co-workers achieved this by activating the metal complex in methanol and subsequently added water to the sample prior to removal of methanol in a 40 °C water bath.[65] This method delivered 1% ^{1}H-polarization for 3-amino-1,2,4-triazine, however analysis of the final solvent composition revealed up to 10% residual methanol. A similar strategy has been reported whereby the catalyst was activated in ethanol-d_6 and the solvent removed *before* the addition of D_2O.[66] Again, this chemical change renders the active catalyst water soluble and led to SABRE induced ^{1}H-signal enhancements of ≈30-fold in nicotinamide at 9.4 T.

To avoid the pre-activation in an organic solvent, water-soluble SABRE catalysts were developed as shown in Figures 6 and 7. Firstly, the use of an ancillary phosphine ligand that is functionalized with hydrophilic arylsulfonates (**4**) led to aqueous solubility.[67] Another approach introduced a diol moiety to the COD ligand (**5**) allows the pre-catalyst to be dissolved in water and, despite the removal of this group during the activation process, the activated SABRE catalyst remains in aqueous solution.[68] This gave up to 32-fold ^{1}H-enhancments for pyridine at 9.4 T.

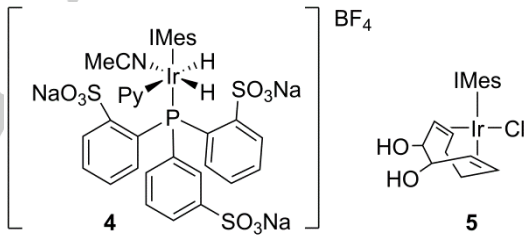

Figure 6. Structure of water soluble SABRE catalysts containing co-ligands

Alternative strategies have concentrated on modification of the NHC ligand, whereby the introduction of a pendant choline moiety (**6**)[67] or using PEGylated groups renders the precatalyst water soluble.[68-69] The pre-catalyst [IrCl(COD)(IDEG)] (**7**) showed most promise and gave up to 42-fold ^{1}H-enhancement at 7 T across a number of substrates and ≈1000-fold ^{15}N-enhancement at (7 T) for ^{15}N-pyridine, however, catalyst removal would still be necessary to create a biocompatible bolus for *in vivo* injection.[70]

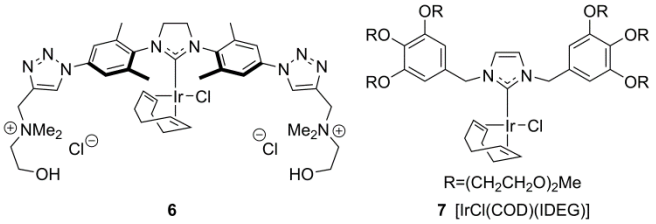

Figure 7. Structure of water soluble NHC ligands used for SABRE catalysis

7.2. Heterogeneous SABRE

Heterogeneous SABRE also reflects a potential route to create a biocompatible bolus as the catalyst could be easily removed. Heterogeneous catalysis has been widely applied in PHIP and DNP methods previously.[71] For SABRE, the immobilized iridium-NHC catalyst on micropolymer beads (**8**) gave ≈5-fold ^{1}H-enhancment at 9.4 T for the *ortho*- protons of pyridine using SABRE (Figure 8).[72] This enhancement, despite being low, was shown to be achieved only from the heterogeneous catalysis by comparison to control experiments on the supernatant solution. Alternatively, an iridium-NHC catalyst immobilized on silica gel (**9**) led to a 100-fold ^{15}N-enhancement at 9.4 T in ^{15}N-pyridine after polarization transfer at low magnetic fields in methanol.[73]

Currently, neither heterogeneous SABRE nor aqueous SABRE deliver polarization levels that are commensurate with biomedical imaging. Additionally, the heterogeneous catalysis has only been reported in methanol solutions which are not biocompatible and thus, further development is required before this high potential technique can be realized for *in vivo* applications.

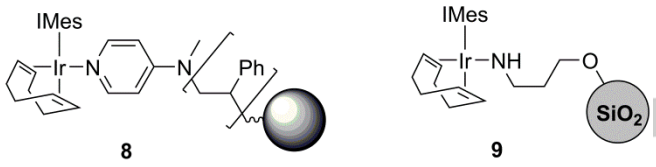

Figure 8. Heterogeneous SABRE catalysts

7.3. Biphasic SABRE catalysis

A facile route to produce a potentially biocompatible bolus for *in vivo* investigation has been reported through the use of biphasic catalysis. This allows the catalyst to remain in the organic phase and the aqueous phase, containing the hyperpolarized substrate, can be separated as previously established for PHIP.[8, 71f] Biphasic SABRE catalysis, dubbed CAtalyst Separated Hyperpolarization *via* Signal Amplification by Reversible Exchange (CASH-SABRE), has been exemplified using 0.3 mL of $CDCl_3$ containing 5 mM of [IrCl(COD)(IMes)] and 0.3 mL of D_2O containing 20-100 mM of the hyperpolarization target and 0.16 w/v% NaCl.[74] This led to up to 3000-fold signal enhancement at 9.4 T when using methyl 4,6-d_2-nicotinate. Importantly, just 1.5 x 10^{-6} M of the iridium catalyst and 0.06% $CDCl_3$ contamination in the aqueous phase was observed. This method has been exemplified with a number of substrates and images showing the hyperpolarized material in the aqueous phase were described.

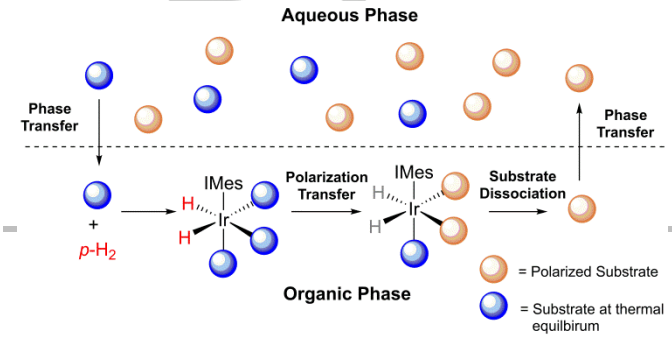

Figure 9. Schematic representation of biphasic SABRE catalysis.

8. Summary and Outlook

In summary, SABRE is a simple hyperpolarization technique that brings together many different approaches of magnetic resonance, synthetic chemistry and catalysis. There is a need to understand all of these components if very high polarization levels are to be achieved more generally. At the heart of the SABRE process is the metal catalyst that mediates polarization transfer and modifying the catalyst has caused significant improvements in SABRE efficacy. This polarization technique has been applied to a range of nuclei and has begun to improve a number of analytical methods. The key breakthrough for application of the SABRE technique in a clinical setting will be the observation of a polarized substrate *in vivo* and this could open the door to studying disease models in real time.

Finally, whilst it is established that ^{1}H and spin-½ heteronuclei can be readily sensitized by SABRE, the range of molecules is limited by the necessity to bind to the metal center; only aromatic heterocycles, nitriles, Schiff bases and diazirines currently feature regularly. Thus, harnessing *p*-H_2 more widely will be the key to the future development of SABRE, particularly with the proven use of pyruvate, glucose and urea in *in vivo* DNP studies.

Overcoming the requirement for binding the target substrate to the metal catalyst has recently been achieved using a technique that has been named SABRE-RELAY.[75] This method begins by using SABRE to hyperpolarize an amine or ammonia and proton exchanges allows the relay of polarization into the target substrate (Scheme 2). ^{1}H NMR signal gains of up to 650-fold per proton were reported in conjunction with ^{13}C signal enhancements at 9.4 T of 570-fold for 1-propanol. Importantly, the simple polarization of ^{1}H ^{13}C, ^{31}P and ^{15}N nuclei in a range of amide, alcohol, carboxylic acid, phosphate and carbonate substrates was exemplified. Moreover, as this methodology gives access to hyperpolarized pyruvate, glucose and urea, with development it may ultimately reflect a cost efficient alternative to DNP. We predict that the advent of SABRE-RELAY will greatly increase the range of *p*-H_2 based hyperpolarization applications in the future and encourage a far greater array of researchers to contribute to these developments.

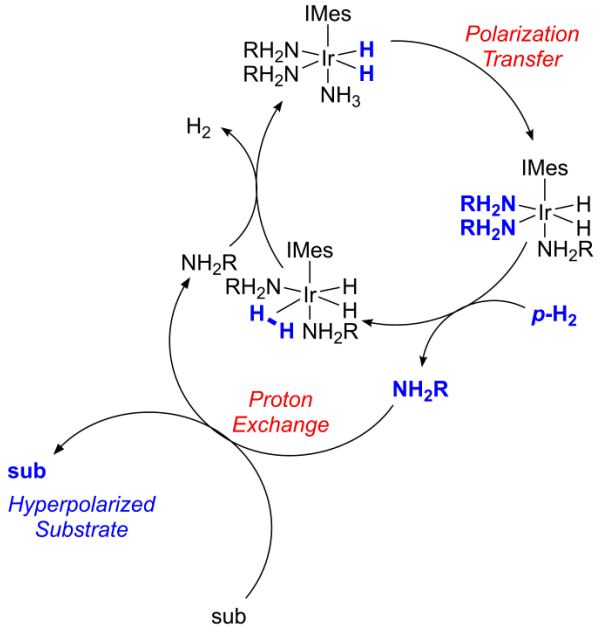

Scheme 2. Schematic representation for the SABRE-RELAY process in which an amine or ammonia is polarized and then subsequently relays its polarization to a target substrate (sub) *via* proton exchange.

Acknowledgements

We thank the Wellcome Trust (092506 and 098335) for funding.

Keywords: SABRE • hyperpolarization • NMR • MRI • catalysis

[1] (a) J. Kurhanewicz, D. B. Vigneron, K. Brindle, E. Y. Chekmenev, A. Comment, C. H. Cunningham, R. J. DeBerardinis, G. G. Green, M. O. Leach, S. S. Rajan, R. R. Rizi, B. D. Ross, W. S. Warren, C. R. Malloy, *Neoplasia* **2011**, *13*, 81-97; (b) K. R. Keshari, D. M. Wilson, *Chem. Soc. Rev.* **2014**, *43*, 1627-1659; (c) S. J. Nelson, J. Kurhanewicz, D. B. Vigneron, P. E. Z. Larson, A. L. Harzstark, M. Ferrone, M. van Criekinge, J. W. Chang, R. Bok, I. Park, G. Reed, L. Carvajal, E. J. Small, P. Munster, V. K. Weinberg, J. H. Ardenkjaer-Larsen, A. P. Chen, R. E. Hurd, L.-I. Odegardstuen, F. J. Robb, J. Tropp, J. A. Murray, *Sci. Transl. Med.* **2013**, *5*, 198ra108; (d) T. B. Rodrigues, E. M. Serrao, B. W. C. Kennedy, D.-E. Hu, M. I. Kettunen, K. M. Brindle, *Nat Med* **2014**, *20*, 93-97; (e) H. Gutte, A. E. Hansen, H. H. Johannesen, A. E. Clemmensen, J. H. Ardenkjær-Larsen, C. H. Nielsen, A. Kjær, *Am. J. Nucl Med. Mol. Imaging* **2015**, *5*, 548-560; (f) J. H. Ardenkjær-Larsen, B. Fridlund, A. Gram, G. Hansson, L. Hansson, M. H. Lerche, R. Servin, M. Thaning, K. Golman, *Proc. Natal. Acad. Sci.* **2003**, *100*, 10158-10163; (g) C. H. Cunningham, J. Y. C. Lau, A. P. Chen, B. J. Geraghty, W. J. Perks, I. Roifman, G. A. Wright, K. A. Connelly, *Circulation Research* **2016**, *119*, 1177-1182.

[2] P. Nikolaou, A. M. Coffey, L. L. Walkup, B. M. Gust, N. Whiting, H. Newton, I. Muradyan, M. Dabaghyan, K. Ranta, G. D. Moroz, M. S. Rosen, S. Patz, M. J. Barlow, E. Y. Chekmenev, B. M. Goodson, *Magnetic Resonance Imaging* **2014**, *32*, 541-550.

[3] L. Frydman, *Nature Chemistry* **2009**, *1*, 176-178.

[4] (a) V. Daniele, F. X. Legrand, P. Berthault, J. N. Dumez, G. Huber, *Chemphyschem* **2015**, *16*, 3413-3417; (b) J.-N. Dumez, J. Milani, B. Vuichoud, A. Bornet, J. Lalande-Martin, I. Tea, M. Yon, M. Maucourt, C. Deborde, A. Moing, L. Frydman, G. Bodenhausen, S. Jannin, P. Giraudeau, *Analyst* **2015**, *140*, 5860-5863; (c) N. K. J. Hermkens, N. Eshuis, B. J. A. van Weerdenburg, M. C. Feiters, F. P. J. T. Rutjes, S. S. Wijmenga, M. Tessari, *Anal. Chem.* **2016**, *88*, 3406-3412; (d) I. Reile, N. Eshuis, N. K. J. Hermkens, B. J. A. van Weerdenburg, M. C. Feiters, F. Rutjes, M. Tessari, *Analyst* **2016**, *141*, 4001-4005; (e) N. Eshuis, N. Hermkens, B. J. A. van Weerdenburg, M. C. Feiters, F. Rutjes, S. S. Wijmenga, M. Tessari, *J. Am. Chem. Soc.* **2014**, *136*, 2695-2698; (f) N. Eshuis, R. Aspers, B. J. A. van Weerdenburg, M. C. Feiters, F. Rutjes, S. S. Wijmenga, M. Tessari, *Angew. Chem. Int. Ed.* **2015**, *54*, 14527-14530.

[5] (a) S. Wildschütz, P. Hübler, J. Bargon, *ChemPhysChem* **2001**, *2*, 328-331; (b) D. Guan, A. Jonathan Holmes, J. Lopez-Serrano, S. B. Duckett, *Catalysis Science & Technology* **2017**, *7*, 2101-2109; (c) S. B. Duckett, N. J. Wood, *Coord. Chem. Rev.* **2008**, *252*, 2278-2291; (d) J. Lopez-Serrano, S. B. Duckett, J. P. Dunne, C. Godard, A. C. Whitwood, *Dalton Trans.* **2008**, 4270-4281.

[6] C. R. Bowers, D. P. Weitekamp, *J. Am. Chem. Soc.* **1987**, *109*, 5541-5542.

[7] R. A. Green, R. W. Adams, S. B. Duckett, R. E. Mewis, D. C. Williamson, G. G. R. Green, *Prog. Nucl. Magn. Reson. Spectrosc.* **2012**, *67*, 1-48.

[8] (a) F. Reineri, T. Boi, S. Aime, *Nat. Commun.* **2015**, *6*, 5858; (b) E. Cavallari, C. Carrera, S. Aime, F. Reineri, *Chem. Eur. J.* **2017**, *23*, 1200-1204.

[9] R. W. Adams, J. A. Aguilar, K. D. Atkinson, M. J. Cowley, P. I. P. Elliott, S. B. Duckett, G. G. R. Green, I. G. Khazal, J. López-Serrano, D. C. Williamson, *Science* **2009**, *323*, 1708-1711.

[10] R. W. Adams, S. B. Duckett, R. A. Green, D. C. Williamson, G. G. R. Green, *J. Chem. Phys.* **2009**, *131*.

[11] A. N. Pravdivtsev, A. V. Yurkovskaya, H. M. Vieth, K. L. Ivanov, R. Kaptein, *Chemphyschem* **2013**, *14*, 3327-3331.

[12] (a) K. D. Atkinson, M. J. Cowley, S. B. Duckett, P. I. P. Elliott, G. G. R. Green, J. López-Serrano, I. G. Khazal, A. C. Whitwood, *Inorg. Chem.* **2009**, *48*, 663-670; (b) A. N. Pravdivtsev, A. V. Yurkovskaya, H. M. Vieth, K. L. Ivanov, *J. Phys. Chem. B* **2015**, *119*, 13619-13629; (c) T. Theis, M. Truong, A. M. Coffey, E. Y. Chekmenev, W. S. Warren, *J. Mag. Res.* **2014**, *248*, 23-26.

[13] (a) K. L. Ivanov, A. N. Pravdivtsev, A. V. Yurkovskaya, H. M. Vieth, R. Kaptein, *Prog. Nucl. Magn. Reson. Spectrosc.* **2014**, *81*, 1-36; (b) D. A. Barskiy, A. N. Pravdivtsev, K. L. Ivanov, K. V. Kovtunov, I. V. Koptyug, *Phys. Chem. Chem. Phys.* **2016**, *18*, 89-93; (c) S. Knecht, A. N. Pravdivtsev, J.-B. Hovener, A. V. Yurkovskaya, K. L. Ivanov, *RSC Advances* **2016**, *6*, 24470-24477.

[14] A. J. Holmes, P. J. Rayner, M. J. Cowley, G. G. R. Green, A. C. Whitwood, S. B. Duckett, *Dalton Trans.* **2015**, *44*, 1077-1083.

[15] N. Eshuis, R. Aspers, B. J. A. van Weerdenburg, M. C. Feiters, F. Rutjes, S. S. Wijmenga, M. Tessari, *J. Mag. Res.* **2016**, *265*, 59-66.

[16] K. D. Atkinson, M. J. Cowley, P. I. P. Elliott, S. B. Duckett, G. G. R. Green, J. López-Serrano, A. C. Whitwood, *J. Am. Chem. Soc.* **2009**, *131*, 13362-13368.

[17] M. J. Cowley, R. W. Adams, K. D. Atkinson, M. C. R. Cockett, S. B. Duckett, G. G. R. Green, J. A. B. Lohman, R. Kerssebaum, D. Kilgour, R. E. Mewis, *J. Am. Chem. Soc.* **2011**, *133*, 6134-6137.

[18] L. S. Lloyd, A. Asghar, M. J. Burns, A. Charlton, S. Coombes, M. J. Cowley, G. J. Dear, S. B. Duckett, G. R. Genov, G. G. R. Green, L. A. R. Highton, A. J. J. Hooper,

M. Khan, I. G. Khazal, R. J. Lewis, R. E. Mewis, A. D. Roberts, A. J. Ruddlesden, *Catalysis Science & Technology* **2014**, *4*, 3544-3554.
[19] B. J. A. van Weerdenburg, S. Gloggler, N. Eshuis, A. H. J. Engwerda, J. M. M. Smits, R. de Gelder, S. Appelt, S. S. Wymenga, M. Tessari, M. C. Feiters, B. Blumich, F. Rutjes, *Chem. Commun.* **2013**, *49*, 7388-7390.
[20] M. Fekete, P. J. Rayner, G. G. R. Green, S. B. Duckett, *Magn. Reson. Chem.* **2017**, 10.1002/mrc.4607.
[21] S. V. C. Vummaleti, D. J. Nelson, A. Poater, A. Gomez-Suarez, D. B. Cordes, A. M. Z. Slawin, S. P. Nolan, L. Cavallo, *Chem. Sci.* **2015**, *6*, 1895-1904.
[22] B. J. A. van Weerdenburg, N. Eshuis, M. Tessari, F. Rutjes, M. C. Feiters, *Dalton Trans.* **2015**, *44*, 15387-15390.
[23] (a) A. J. Ruddlesden, R. E. Mewis, G. G. R. Green, A. C. Whitwood, S. B. Duckett, *Organometallics* **2015**, *34*, 2997-3006; (b) M. Fekete, O. Bayfield, S. B. Duckett, S. Hart, R. E. Mewis, N. Pridmore, P. J. Rayner, A. Whitwood, *Inorg. Chem.* **2013**, *52*, 13453-13461.
[24] W. Iali, G. G. R. Green, S. J. Hart, A. C. Whitwood, S. B. Duckett, *Inorg. Chem.* **2016**, *55*, 11639-11643.
[25] E. B. Ducker, L. T. Kuhn, K. Munnemann, C. Griesinger, *J. Mag. Res.* **2012**, *214*, 159-165.
[26] R. E. Mewis, K. D. Atkinson, M. J. Cowley, S. B. Duckett, G. G. R. Green, R. A. Green, L. A. R. Highton, D. Kilgour, L. S. Lloyd, J. A. B. Lohman, D. C. Williamson, *Magn. Reson. Chem.* **2014**, *52*, 358-369.
[27] (a) T. Theis, M. L. Truong, A. M. Coffey, R. V. Shchepin, K. W. Waddell, F. Shi, B. M. Goodson, W. S. Warren, E. Y. Chekmenev, *J. Am. Chem. Soc.* **2015**, *137*, 1404-1407; (b) M. L. Truong, T. Theis, A. M. Coffey, R. V. Shchepin, K. W. Waddell, F. Shi, B. M. Goodson, W. S. Warren, E. Y. Chekmenev, *J. Phys. Chem. C* **2015**, *119*, 8786-8797.
[28] V. V. Zhivonitko, I. V. Skovpin, I. V. Koptyug, *Chem. Commun.* **2015**, *51*, 2506-2509.
[29] (a) A. N. Pravdivtsev, A. V. Yurkovskaya, N. N. Lukzen, H. M. Vieth, K. L. Ivanov, *Phys. Chem. Chem. Phys.* **2014**, *16*, 18707-18719; (b) A. N. Pravdivtsev, A. V. Yurkovskaya, H. Zimmermann, H. M. Vieth, K. L. Ivanov, *Chem. Phys. Lett.* **2016**, *661*, 77-82.
[30] G. Stevanato, *J. Mag. Res.* **2017**, *274*, 148-162.
[31] S. S. Roy, G. Stevanato, P. J. Rayner, S. B. Duckett, *J. Mag. Res.* **2017**, *285*, 55-60.
[32] R. E. Mewis, R. A. Green, M. C. R. Cockett, M. J. Cowley, S. B. Duckett, G. G. R. Green, R. O. John, P. J. Rayner, D. C. Williamson, *J. Phys. Chem. B* **2015**, *119*, 1416-1424.
[33] P. J. Rayner, M. J. Burns, A. M. Olaru, P. Norcott, M. Fekete, G. G. R. Green, L. A. R. Highton, R. E. Mewis, S. B. Duckett, *Proc. Natal. Acad. Sci.* **2017**, *114*, E3188-E3194.
[34] Q. Wang, K. Shen, A. W. J. Logan, J. F. P. Colell, J. Bae, G. X. Ortiz Jr, T. Theis, W. S. Warren, S. J. Malcolmson, *Angew. Chem. Int. Ed.* **2017**, *56*, 12112.
[35] P. Norcott, P. J. Rayner, G. G. R. Green, S. B. Duckett, *Chem. Eur. J.* **2017**, *23*, 16990-16997.
[36] R. E. Mewis, M. Fekete, G. G. R. Green, A. C. Whitwood, S. B. Duckett, *Chem. Commun.* **2015**, *51*, 9857-9859.
[37] R. V. Shchepin, D. A. Barskiy, A. M. Coffey, B. M. Goodson, E. Y. Chekmenev, *Chemistryselect* **2016**, *1*, 2552-2555.
[38] K. M. Appleby, R. E. Mewis, A. M. Olaru, G. G. R. Green, I. J. S. Fairlamb, S. B. Duckett, *Chem. Sci.* **2015**, *6*, 3981-3993.
[39] A. M. Olaru, M. J. Burns, G. G. R. Green, S. B. Duckett, *Chem. Sci.* **2017**, *8*, 2257-2266.
[40] J. B. Hovener, N. Schwaderlapp, T. Lickert, S. B. Duckett, R. E. Mewis, L. A. R. Highton, S. M. Kenny, G. G. R. Green, D. Leibfritz, J. G. Korvink, J. Hennig, D. von Elverfeldt, *Nat. Commun.* **2013**, *4*.
[41] H. F. Zeng, J. D. Xu, J. Gillen, M. T. McMahon, D. Artemov, J. M. Tyburn, J. A. B. Lohman, R. E. Mewis, K. D. Atkinson, G. G. R. Green, S. B. Duckett, P. C. M. van Zijl, *J. Mag. Res.* **2013**, *237*, 73-78.
[42] H. Allouche-Arnon, M. H. Lerche, M. Karlsson, R. E. Lenkinski, R. Katz-Brull, *Contrast Media & Molecular Imaging* **2011**, *6*, 499-506.
[43] J. B. Hovener, N. Schwaderlapp, R. Borowiak, T. Lickert, S. B. Duckett, R. E. Mewis, R. W. Adams, M. J. Burns, L. A. R. Highton, G. G. R. Green, A. Olaru, J. Hennig, D. von Elverfeldtt, *Anal. Chem.* **2014**, *86*, 1767-1774.
[44] M. Carravetta, M. H. Levitt, *J. Am. Chem. Soc.* **2004**, *126*, 6228-6229.
[45] A. M. Olaru, S. S. Roy, L. S. Lloyd, S. Coombes, G. G. R. Green, S. B. Duckett, *Chem. Commun.* **2016**, *52*, 7842-7845.
[46] S. S. Roy, P. J. Rayner, P. Norcott, G. G. R. Green, S. B. Duckett, *Phys. Chem. Chem. Phys.* **2016**, *18*, 24905-24911.
[47] S. S. Roy, P. Norcott, P. J. Rayner, G. G. R. Green, S. B. Duckett, *Angew. Chem. Int. Ed.* **2016**, *55*, 15642-15645.
[48] T. Theis, M. P. Ledbetter, G. Kervern, J. W. Blanchard, P. J. Ganssle, M. C. Butler, H. D. Shin, D. Budker, A. Pines, *J. Am. Chem. Soc.* **2012**, *134*, 3987-3990.
[49] (a) J. F. P. Colell, A. W. J. Logan, Z. J. Zhou, R. V. Shchepin, D. A. Barskiy, G. X. Ortiz, Q. Wang, S. J. Malcolmson, E. Y. Chekmenev, W. S. Warren, T. Theis, *J. Phys. Chem. C* **2017**, *121*, 6626-6634; (b) R. V. Shchepin, D. A. Barskiy, A. M. Coffey, T. Theis, F. Shi, W. S. Warren, B. M. Goodson, E. Y. Chekmenev, *Acs Sensors* **2016**, *1*, 640-644; (c) R. V. Shchepin, D. A. Barskiy, D. M. Mikhaylov, E. Y. Chekmenev, *Bioconjugate Chem.* **2016**, *27*, 878-882.
[50] A. W. J. Logan, T. Theis, J. F. P. Colell, W. S. Warren, S. J. Malcolmson, *Chem. Eur. J.* **2016**, *22*, 10777-10781.
[51] T. Theis, G. X. Ortiz, A. W. J. Logan, K. E. Claytor, Y. Feng, W. P. Huhn, V. Blum, S. J. Malcolmson, E. Y. Chekmenev, Q. Wang, W. S. Warren, *Sci. Adv.* **2016**, *2*.
[52] D. A. Barskiy, R. V. Shchepin, A. M. Coffey, T. Theis, W. S. Warren, B. M. Goodson, E. Y. Chekmenev, *J. Am. Chem. Soc.* **2016**, *138*, 8080-8083.
[53] R. V. Shchepin, M. L. Truong, T. Theis, A. M. Coffey, F. Shi, K. W. Waddell, W. S. Warren, B. M. Goodson, E. Y. Chekmenev, *J. Phys. Chem. Lett.* **2015**, *6*, 1961-1967.
[54] (a) P. Bhattacharya, E. Y. Chekmenev, W. F. Reynolds, S. Wagner, N. Zacharias, H. R. Chan, R. Bünger, B. D. Ross, *NMR Biomed.* **2011**, *24*, 1023-1028; (b) A. Comment, M. E. Merritt, *Biochemistry* **2014**, *53*, 7333-7357; (c) N. M. Zacharias, H. R. Chan, N. Sailasuta, B. D. Ross, P. Bhattacharya, *J. Am. Chem. Soc.* **2012**, *134*, 934-943.
[55] D. A. Barskiy, R. V. Shchepin, C. P. N. Tanner, J. F. P. Colell, B. M. Goodson, T. Theis, W. S. Warren, E. Y. Chekmenev, *ChemPhysChem* **2017**, *18*, 1493-1498.
[56] S. S. Roy, P. Norcott, P. J. Rayner, G. G. R. Green, S. B. Duckett, *Chem. Eur. J.* **2017**, *23*, 10496-10500.
[57] Z. Zhou, J. Yu, J. F. P. Colell, R. Laasner, A. Logan, D. A. Barskiy, R. V. Shchepin, E. Y. Chekmenev, V. Blum, W. S. Warren, T. Theis, *The Journal of Physical Chemistry Letters* **2017**, *8*, 3008-3014.
[58] M. J. Burns, P. J. Rayner, G. G. R. Green, L. A. R. Highton, R. E. Mewis, S. B. Duckett, *J. Phys. Chem. B* **2015**, *119*, 5020-5027.
[59] R. V. Shchepin, B. M. Goodson, T. Theis, W. S. Warren, E. Y. Chekmenev, *Chemphyschem* **2017**, *18*, 1961-1965.
[60] A. M. Olaru, A. Burt, P. J. Rayner, S. J. Hart, A. C. Whitwood, G. G. R. Green, S. B. Duckett, *Chem. Commun.* **2016**, *52*, 14482-14485.
[61] L. S. Lloyd, R. W. Adams, M. Bernstein, S. Coombes, S. B. Duckett, G. G. R. Green, R. J. Lewis, R. E. Mewis, C. J. Sleigh, *J. Am. Chem. Soc.* **2012**, *134*, 12904-12907.

[62] L. Frydman, T. Scherf, A. Lupulescu, *Proc. Natal. Acad. Sci.* **2002**, *99*, 15858-15862.

[63] N. Eshuis, B. J. A. van Weerdenburg, M. C. Feiters, F. Rutjes, S. S. Wijmenga, M. Tessari, *Angew. Chem. Int. Ed.* **2015**, *54*, 1481-1484.

[64] I. Reile, R. L. E. G. Aspers, J.-M. Tyburn, J. G. Kempf, M. C. Feiters, F. P. J. T. Rutjes, M. Tessari, *Angew. Chem. Int. Ed.* **2017**, *56*, 9174-9177.

[65] H. F. Zeng, J. D. Xu, M. T. McMahon, J. A. B. Lohman, P. C. M. van Zijl, *J. Magn. Reson.* **2014**, *246*, 119-121.

[66] M. L. Truong, F. Shi, P. He, B. Yuan, K. N. Plunkett, A. M. Coffey, R. V. Shchepin, D. A. Barskiy, K. V. Kovtunov, I. V. Koptyug, K. W. Waddell, B. M. Goodson, E. Y. Chekmenev, *J. Phys. Chem. B* **2014**, *118*, 13882-13889.

[67] M. Fekete, C. Gibard, G. J. Dear, G. G. R. Green, A. J. J. Hooper, A. D. Roberts, F. Cisnetti, S. B. Duckett, *Dalton Trans.* **2015**, *44*, 7870-7880.

[68] F. Shi, P. He, Q. A. Best, K. Groome, M. L. Truong, A. M. Coffey, G. Zimay, R. V. Shchepin, K. W. Waddell, E. Y. Chekmenev, B. M. Goodson, *J. Phys. Chem. C* **2016**, *120*, 12149-12156.

[69] P. Spannring, I. Reile, M. Emondts, P. P. M. Schleker, N. K. J. Hermkens, N. G. J. van der Zwaluw, B. J. A. van Weerdenburg, P. Tinnemans, M. Tessari, B. Blumich, F. Rutjes, M. C. Feiters, *Chem. Eur. J.* **2016**, *22*, 9277-9282.

[70] J. F. P. Colell, M. Emondts, A. W. J. Logan, K. Shen, J. Bae, R. V. Shchepin, G. X. Ortiz, P. Spannring, Q. Wang, S. J. Malcolmson, E. Y. Chekmenev, M. C. Feiters, F. P. J. T. Rutjes, B. Blümich, T. Theis, W. S. Warren, *J. Am. Chem. Soc.* **2017**, *139*, 7761-7767.

[71] (a) I. V. Koptyug, K. V. Kovtunov, S. R. Burt, M. S. Anwar, C. Hilty, S.-I. Han, A. Pines, R. Z. Sagdeev, *J. Am. Chem. Soc.* **2007**, *129*, 5580-5586; (b) K. V. Kovtunov, I. E. Beck, V. I. Bukhtiyarov, I. V. Koptyug, *Angew. Chem. Int. Ed.* **2008**, *47*, 1492-1495; (c) K. V. Kovtunov, I. E. Beck, V. V. Zhivonitko, D. A. Barskiy, V. I. Bukhtiyarov, I. V. Koptyug, *Phys. Chem. Chem. Phys.* **2012**, *14*, 11008-11014; (d) M. Roth, P. Kindervater, H.-P. Raich, J. Bargon, H. W. Spiess, K. Münnemann, *Angew. Chem. Int. Ed.* **2010**, *49*, 8358-8362; (e) M. D. Lingwood, T. A. Siaw, N. Sailasuta, O. A. Abulseoud, H. R. Chan, B. D. Ross, P. Bhattacharya, S. Han, *Radiology* **2012**, *265*, 418-425; (f) K. V. Kovtunov, V. V. Zhivonitko, I. V. Skovpin, D. A. Barskiy, O. G. Salnikov, I. V. Koptyug, *J. Phys. Chem. C* **2013**, *117*, 22887-22893.

[72] F. Shi, A. M. Coffey, K. W. Waddell, E. Y. Chekmenev, B. M. Goodson, *Angew. Chem. Int. Ed.* **2014**, *53*, 7495-7498.

[73] K. V. Kovtunov, L. M. Kovtunova, M. E. Gemeinhardt, A. V. Bukhtiyarov, J. Gesiorski, V. I. Bukhtiyarov, E. Y. Chekmenev, I. V. Koptyug, B. Goodson, *Angew. Chem. Int. Ed.* **2017**, *56*, 10433-10437.

[74] S. Duckett, W. Iali, A. M. Olaru, G. G. R. Green, *Chem. Eur. J.* **2017**, *23*, 10491-10495.

[75] W. Iali, P. J. Rayner, S. B. Duckett, *Sci. Adv.* **2018**, **4**:eaa06250.

Layout 1:

MINIREVIEW

Signal Amplification by Reversible Exchange (SABRE) is a hyperpolarization technique that dramatically enhances magnetic resonance signals. This minireview tracks its development since its discovery in 2009 and offers an outlook on its potentially use for both analytic sciences and disease diagnosis.

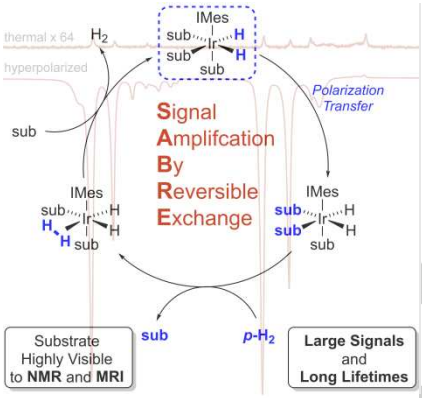

*Peter J. Rayner, Simon B. Duckett**

Page No. – Page No.

Signal Amplification by Reversible Exchange (SABRE): From Discovery to Diagnosis